Wannier function analysis of silicon–carbon alloys

2003 J. Phys.: Condens. Matter 15 165

(http://iopscience.iop.org/0953-8984/15/2/316)

INSTITUTE OF PHYSICS PUBLISHING JOURNAL OF PHYSICS: CONDENSED MATTER

J. Phys.: Condens. Matter **15** (2003) 165–173 PII: S0953-8984(03)38930-1

Wannier function analysis of silicon–carbon alloys

P Fitzhenry, M M M Bilek, N A Marks, N C Cooper and D R McKenzie

School of Physics, The University of Sydney, NSW 2006, Australia

Received 2 July 2002
Published 20 December 2002
Online at stacks.iop.org/JPhysCM/15/165

Abstract

Maximally localized Wannier functions are the basis of a new technique for resolving ambiguous bonding issues for amorphous materials. Geometrical methods using the Wannier function representation provide an insightful chemical picture of local bonding and hybridization in disordered structures. Central to these methods is the notion of treating the Wannier function centres as a virtual atomic species with a well-defined degree of localization. Using Wannier function methods, we classify and quantify the types of bonding present in a sample of the ternary alloy hydrogenated amorphous silicon carbide, $C_{22}Si_{22}H_{20}$. In addition to the bonding previously observed for this material, we see three-centre bonding and flipping bonds. We identify a cluster defect in our sample associated with these flipping bonds, and observe a temperature dependence of the bond flipping. This effect may be observable using temperature-dependent Raman spectroscopy.

(Some figures in this article are in colour only in the electronic version)

1. Introduction

Amorphous silicon–carbon alloys are of technological interest because of their useful electronic and mechanical properties [1]. At low carbon contents, hydrogenated amorphous silicon–carbon alloy films prepared by plasma deposition have comparable carrier mobilities to pure hydrogenated amorphous silicon films prepared in a similar way [2]. The films can also be n- and p-type doped by the addition of impurities such as boron and phosphorus. However, it is found that the electronic band gap and the optical gap are larger and are dependent on the carbon content [3]. Hydrogenation of SiC alloys increases their optical and mobility gaps. An application which uses these characteristics is the p-type top layer of amorphous silicon solar cells where the wider optical gap increases the transparency of the top layer and the larger band gap increases the open-circuit voltage, leading to an increased efficiency [4].

Ab initio molecular dynamics methods, based on density functional theory for the solution of the electron states, are capable of answering questions concerning amorphous network solids that remain unresolved by available experimental techniques. These methods are sufficiently accurate to resolve issues such as the analysis of chemical bonding and the assignment of

vibrational states to particular atomic configurations. In this paper we apply the Car–Parrinello method [5] to synthesize a simulated network structure of the ternary alloy system hydrogenated amorphous silicon carbide (a-SiC:H) using the liquid-quench technique. Through the work of Marzari and Vanderbilt [6] it has become possible to study the bonding in these networks from a localized real-space perspective by using maximally localized generalized Wannier functions. Previous studies of amorphous carbon (a-C) networks [7, 8] have shown the value of first-principles methods in the study of structure in cases where the bonding hybridization is highly variable, while studies of the amorphous silicon (a-Si) structure [9, 10] have shown the value of Wannier function analysis in resolving bonding issues.

2. Computational method

This study uses density functional theory [11, 12] in a generalized gradient approximation [13] using norm-conserving Kleinman–Bylander pseudopotentials [14] as implemented by the Car–Parrinello molecular dynamics (CPMD) electronic structure code [15]. A closed-shell analysis is performed and unpaired spin defects, such as dangling bonds, are not treated. However, these are not expected to have any significant effect on the bonding within the network as the experimental spin density is less than $\approx 10^{19}$ spins cm^{-3} [16]. CPMD was used to study a sample of a-SiC:H consisting of 22 atoms of Si, 22 atoms of C and 20 atoms of H in a simple cubic supercell of side dimension 8.68 Å corresponding to a density of 2.35 g cm^{-3}. The a-SiC:H sample was generated using the liquid-quench method. Constant-temperature simulations were run for 0.5 ps duration at 77, 125, 200 and 300 K.

3. Defining connectivity in an amorphous network

3.1. Conventional approach: atom–atom pair correlation

Inter-species pair correlation functions are usually the starting point in bonding characterization studies of disordered structures. However, this approach is problematic for a-SiC:H where it is not possible to unambiguously define a silicon–silicon nearest-neighbour distance. This situation is illustrated in figure 1 which shows the Si–Si pair correlation function $g(r)$ defined by $g(r) = \rho(r)/\rho_0$ where $\rho(r)$ is the atomic number density at distance r and ρ_0 is the average. Also shown in this figure is the electron density around a structural fragment which is very nearly coplanar. Two key difficulties are identified here. The first is that it is not possible to assign a well-defined nearest-neighbour distance for Si–Si bonding as the partial pair correlation does not vanish in the region between first and second neighbours. The second problem is even more fundamental, in that distance alone does not provide a meaningful bonding criterion, as seen in the electron density plot which shows that the longer Si1–Si2 distance represents a bond, while the shorter Si2–Si3 distance does not.

Returning to the first problem, we note that if we had used the first minimum in $g(r)$ for the cut-off of the first coordination sphere, then both pairs of atoms would be assigned as bonded neighbours, yet the electron density shows this clearly not to be the case. In the language of first and second neighbours, we thus have the situation that the first- and second-neighbour peaks are broadened to such an extent in complex multi-species systems, that definitive cut-off distances in the partial pair correlation functions no longer exist. An impractical alternative would be to manually inspect the electron density of all bonds, but aside from being overwhelmingly time consuming, this still suffers from the difficulty of choosing a density cut-off which defines a bond. We therefore need a new strategy for assigning and determining coordination in these systems.

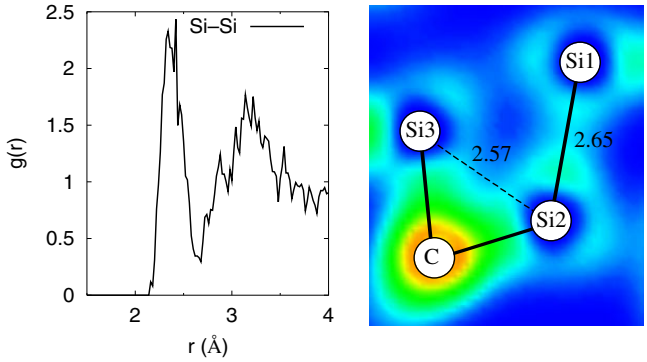

Figure 1. Left: the partial pair correlation function between silicon atoms for the 64-atom a-SiC:H network. Right: the electron density of a fragment of four atoms which are nearly coplanar.

3.2. A Wannier function approach: Wannier atom pair correlation

An alternative approach to determining coordination is based upon a Wannier [6, 17, 18] representation of the occupied Kohn–Sham orbitals. Marzari and Vanderbilt [6] have shown that minimizing the total real-space spread of the Wannier functions w_n uniquely defines a unitary transformation relating the Wannier functions and the Kohn–Sham orbitals. Wannier function centres (WFCs) [19] are then defined as the expectation value of the position operator acting on each individual Wannier function. These WFCs can then be treated as a virtual species for the purposes of coordination analysis. Associated with each WFC is a localization parameter $\sigma_n = \sqrt{\langle r^2\rangle_n - \langle \boldsymbol{r}_n^2\rangle}$ which provides a measure of the real-space spread of the corresponding Wannier function $w_n(\boldsymbol{r})$. This approach was first applied in studies of defects in amorphous silicon [9, 10]. In this work the use of WFCs is extended to a complex, multi-component system, where first- and second-neighbour shells overlap.

The partial pair correlation functions $g_w(r)$ between the WFCs and each atomic species (figure 2) show a clear separation between the first- and second-'neighbour' peaks. This is in marked contrast to the case in figure 1 where the first- and second-neighbour shells overlap significantly. The only exception is for silicon, where there is a very minor contribution around 1.65 Å due to time fluctuation of the bonding. The effect of this on $g_w(r)$ is seen in the lower-right panel of figure 2 and will be discussed further in section 4. Inspection of figure 2 also reveals small peaks in the carbon and silicon partial correlation functions. These peaks indicate the presence of anomalous bonding in the form of lone pairs and three-centre bonds. Such information is not available from conventional atom–atom pair correlation functions.

3.3. Wannier function-based definition of a chemical bond

While there is no well-accepted definition of a chemical bond in a disordered system, the clear nearest-neighbour cut-off distances between the WFCs and the other atoms in this system give a criterion that does not depend *directly* on the inter-atomic distance. Two atoms can then be regarded as chemically bonded when a WFC lies within a so-called *association length* for the respective atomic species. The WFC acts as a link between the atoms, indicating the presence of a chemical bond. Using figure 2 we define the Wannier association lengths to be 0.75 Å for H, 1.10 Å for C and 1.65 Å for Si. This definition of Wannier coordination is used for the remainder of this paper.

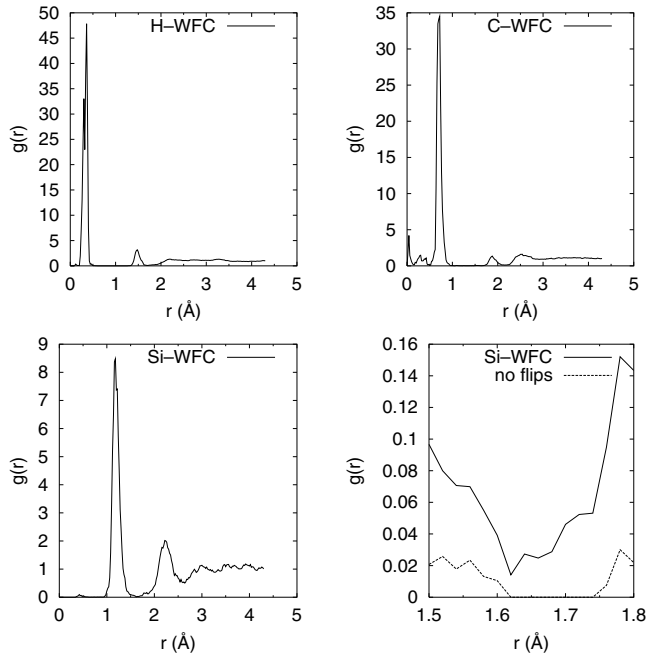

Figure 2. Pair correlation functions $g_w(r)$ for WFCs with atomic species in a-SiC:H at 300 K. The lower-right figure shows the effect of ignoring distances affected by the movement or 'flipping' of a WFC.

The majority of the WFCs are associated with two atoms, but a couple of other configurations are present. One of these is the lone pair, in which a WFC is associated with a single atom. Another important configuration is the three-atom complex, where the WFC lies within the respective association lengths of three atoms, as has been documented for a-Si by Fornari *et al* [10]. An example of such a fragment in our system is shown in figure 3(b). The chemically intuitive preferred interpretation is to define bonds between the atom pairs Si1–C1 and C1–C2 but not between Si1 and C2 as the separation of 2.7 Å is some 40% longer than a usual Si–C bond. This definition is supported by the Wannier analysis of the molecule diborane (figure 3(a)), in which the H atoms are seen to form B–H–B bridging bonds joining the two BH_2 groups. Thus in the context of a WFC definition of chemical bonding, the atom closest to the WFC is chemically bonded to the other two atoms. However, the two atoms furthest from the WFC are not considered to be bonded to each other. This rule of association is used for all three-atom WFCs in this paper.

4. Mobility of Wannier function centres

For the a-SiC:H system a number of the WFCs are highly mobile and at times highly delocalized. Some of these exhibit a flipping behaviour, whereby the WFC changes the set of atoms that it is associated with over time. Figure 4 presents two examples of this behaviour, showing sequences taken from CPMD simulations at 300 K. In panels (a)–(c) a WFC initially associated with an Si atom and an H atom breaks the link to become a lone pair and then later forms a new link between two Si atoms. The temporal spacing between the frames is 0.14 fs/frame. In panels (d)–(f) a WFC initially associated with two C atoms as part of a

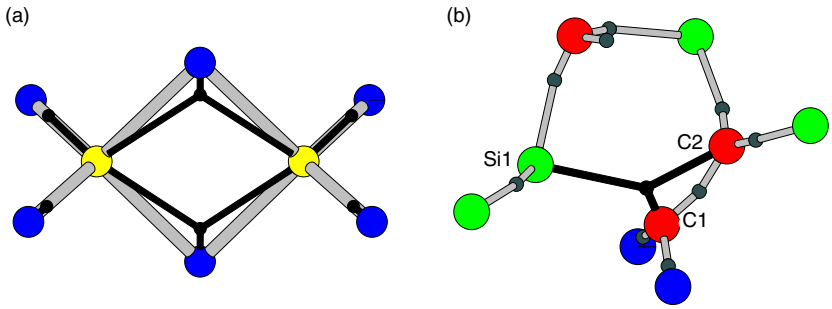

Figure 3. (a) The diborane (B_2H_6) molecule, showing the role of three-atom WFCs in the formation of the B–H–B bridging bonds. B atoms are light circles, H atoms are dark circles and WFCs are shown as small black dots. Atom–atom bonds are shown in grey to illustrate the accepted interpretation of the chemical bonding in diborane. (b) A typical three-centre WFC in a-SiC:H at 300 K. Si atoms are light grey, C atoms are dark grey, H atoms are black and the WFCs are shown as small black dots. The three-centre WFC links are highlighted in black for clarity.

double bond breaks the link to form a bond between a C atom and a Si atom and then later returns to linking the original two C atoms. Here the temporal spacing is 3.5 fs/frame.

These mobile WFCs contribute a small signal in the atom–WFC pair correlation functions seen earlier in figure 2, and the probability density does not drop identically to zero between the first two principal peaks of Si. However, when the atoms involved in flipping events are excluded, an unambiguous zero-region is present, and thus a well-defined association length can be assigned for Si.

4.1. Temperature dependence

By examining the simulations over time, two types of flipping behaviour were identified. The first occurs when WFCs oscillate close to the bond association lengths of two atoms belonging to a strained cluster complex. Motion of the WFCs leads to WFC–atom distances falling on both sides of the bonding association distance, thus produces a flipping effect but no significant change in bonding. This effect is dominant at low temperature, where there is insufficient thermal energy to activate the migration of the WFC.

The second type of flipping occurs when a WFC moves definitively into the sphere of one particular strained group and alleviates the strain there by forming a metastable bond. If this reduces the total strain in the network, then the WFC will stay there. However, if there is another strained subsystem nearby, it may capture the WFC again at some later time. This annealing effect increases flipping at high temperature.

The oscillations which are trivial (in that they do not produce true changes in bonding) dominate at low temperature. Table 1 shows the number of flips executed by two selected WFCs as a function of temperature. WFC1 shows the behaviour characteristic of a mobile WFC and shows an increasing number of flips as temperature increases. WFC2 (also seen in figures 4(d)–(f)) shows the trivial flipping produced by small oscillations at low temperature. This type of flipping decreases with increasing temperature as strain in the network is relaxed. The number of WFCs engaged in flipping behaviour generally increases with temperature as shown in table 2. However, even at the highest temperatures considered, only 8% of the WFCs are involved in flipping events.

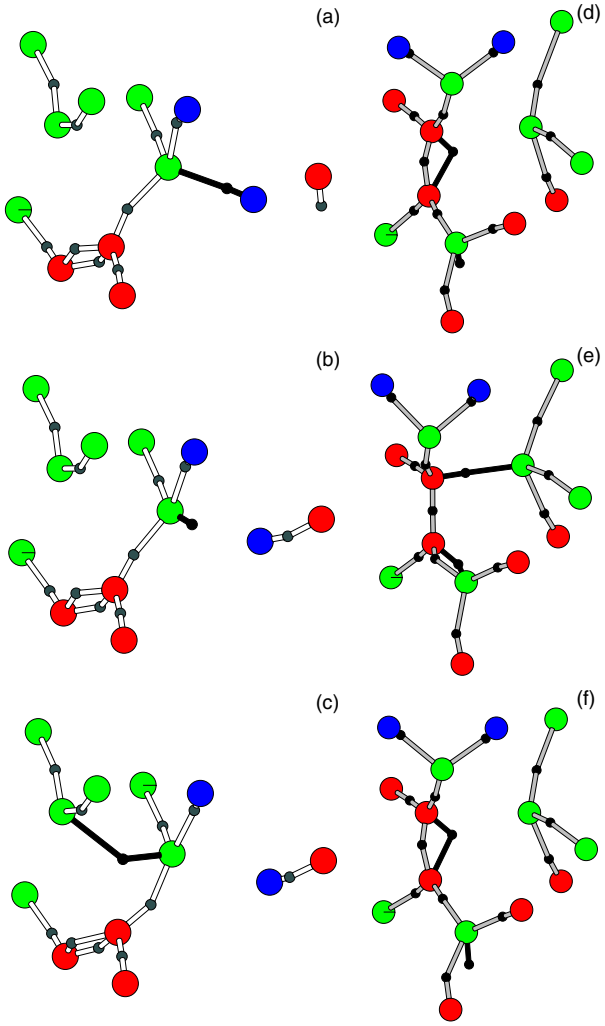

Figure 4. Flipping WFCs at 300 K. The temporal spacing for panels (a)–(c) is 0.14 fs/frame. The temporal spacing for panels (d)–(f) is 3.5 fs/frame. Si atoms are shown as light grey, C atoms are shown as dark grey, H atoms are shown as black and WFCs are shown as small dots.

Table 1. Number of raw flips for two individual WFCs as a function of temperature. WFC1 is a typical mobile WFC, while WFC2 is a typical trivial oscillating WFC.

	77 K	125 K	200 K	300 K
WFC1:	7	9	12	13
WFC2:	7	12	4	4

4.2. A cluster defect identified

In a-SiC:H the flipping bonds are associated with atomic clusters consisting of either an sp^2 hybridized C–C pair or an sp^2 hybridized C–Si pair. Flipping then occurs with a satellite atom

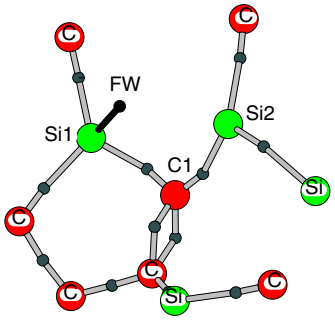

Figure 5. An extended defect in a-SiC:H at 300 K. The defect group is associated with WFC bond flipping. Flipping occurs between Si1, C1 and Si2. Si atoms are light grey, C atoms are dark grey and WFCs are black.

Table 2. Numbers of WFCs involved in flipping at different temperatures.

	77 K	125 K	200 K	300 K
Number of WFCs involved in flipping	2	2	6	8
Total number of flipping events	15	24	36	59

that is usually directly associated with one member of the pair. Extended defects such as this have been noted previously in a-Si [10].

A typical example of this extended defect is shown in figure 5. Both Si1 and Si2 in figure 5 alternate between under-coordination, generally labelled in the literature as T_3, and normal coordination, similarly labelled as T_4. The WFC labelled FW is the one which flips, alternately forming the linkages Si2–C1, Si1–Si2 and Si1–C1–Si2.

4.3. Mobility and localization

The WFC localization parameter σ_n is also time dependent. Analysis of the 98 WFCs showed that the WFC mobility and fluctuations in localization are correlated, with the WFC becoming highly delocalized during a mobility event. To illustrate this correlation a deviation parameter was defined using $\mathrm{d}s_n = |w_n(t + \Delta t) - w_n(t)|$ where $\Delta t = 0.36$ fs is the WFC sampling rate. The left panel in figure 6 is a typical example of an unstable WFC which has a large average localization ($\sigma_{av} = 1.7$ Å), with the greatest delocalization seen around $t = 400$ fs where the two large spikes in the deviation parameter $\mathrm{d}s$ indicate significant changes in the position of the WFC.

In contrast, the right panel in figure 6 shows the localization and $\mathrm{d}s$ for an inactive WFC. In this case the deviation per time step $\mathrm{d}s$ of the WFC is very small, indicating a stable WFC. Similarly, the localization is also smaller, which an average value of 0.88 Å. An interesting feature of the stable WFC is the regular periodic fluctuation in $\sigma(t)$. The shorter period of oscillation was determined to be 12 fs, corresponding to a wavenumber of $\approx$3000 cm^{-1}. This is very similar to the stretch mode in C–H bonds, and inspection of the structure showed this particular WFC is indeed associated with a H and a C atom. The longer-period oscillations, measured at $\approx$150 fs, correspond to a wavenumber of $\approx$200 cm^{-1}. This WFC is associated with a C atom forming part of a dihydride and inspection of an animated sequence of the simulation suggests that this lower-frequency oscillation is associated with a wagging of the CH_2 group.

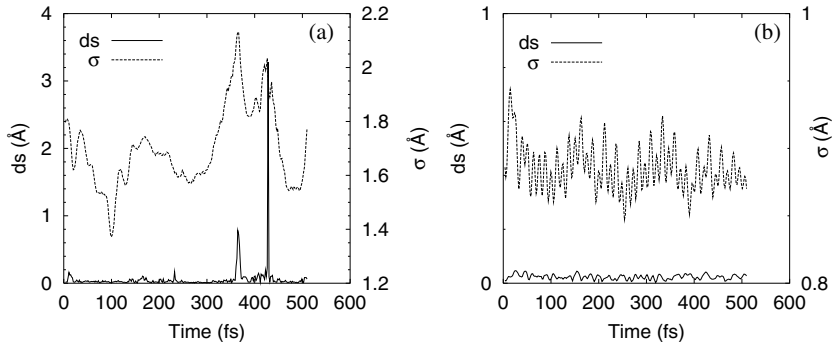

Figure 6. Plots of the deviation parameter ds, and the localization parameter σ_n, at 300 K for (a) a delocalized WFC involved in bond flipping and (b) a stable WFC associated with a C atom and a H atom.

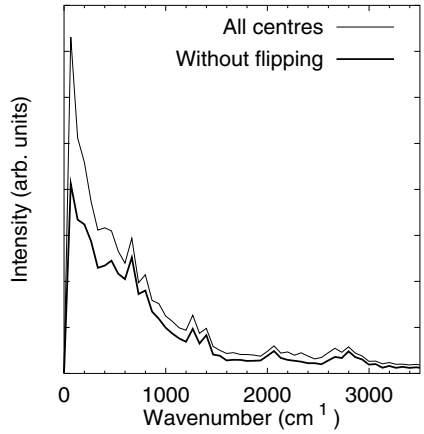

Figure 7. The frequency spectrum of the localization parameter σ. The thin curve shows the spectrum for all WFCs, while the thick curve excludes the flipping WFCs.

It may be possible to observe these flipping rates experimentally using Raman spectroscopy. The Raman spectrum results from a modulation of the polarizability of a specimen through atomic motion. This changing polarizability modulates re-radiated light, producing the Stokes and anti-Stokes Raman lines. As the electronic states in a-SiC:H are strongly modified by the flipping process, there should be a signature in the Raman spectrum. Frequencies characteristic of the Raman spectrum should agree with those that appear in the frequency spectrum of the WFC localization parameter. Such spectra calculated for our a-SiC:H structure are shown in figure 7. The thin curve shows the spectrum for all WFCs, while the thick curve excludes the flipping WFCs. Note that the small number of flipping centres ($\approx$8%) contribute almost half of the low-frequency peak.

5. Conclusions

The use of WFCs is a convenient way of representing the local electron density distribution and allows a simple definition of a chemical bond based on geometric considerations only. The localization and decay properties of the Wannier functions were used to create a virtual

atomic species in the system. Standard geometrical and statistical analysis was then applied to the ensemble of atoms plus WFCs.

This method was applied to the ternary alloy a-SiC:H for which an inter-atomic distance-based coordination analysis gives results inconsistent with the electron density distribution. Using molecular dynamics simulations, we observed that the WFCs were identified with different atoms at different times, indicating that bonds were being made and broken continuously due to the thermal motion of the atoms. This bond flipping correlated with increases in the localization quantity which measures the spatial extent of the local electronic function. The frequency spectrum of the localization showed a large contribution at low frequencies below 100 cm^{-1} from the flipping WFCs. We predict that, because the flipping process is temperature dependent, there should be a characteristic temperature-dependent Raman signature in this frequency range.

References

[1] Bullot J and Schmidt M P 1987 *Phys. Status Solidi* b **143** 345
[2] Chew K, Rusli, Yu M B, Yoon S F, Ligatchev V and Ahn J 2001 *Diamond Relat. Mater.* **10** 1273
[3] Tobata A, June Y, Suzuoki Y and Muzutani T 1997 *J. Phys. D: Appl. Phys.* **30** 194
[4] Tawada Y, Kondo M, Okamoto H and Hamakawa Y 1982 *Sol. Energy Mater.* **6** 299
[5] Car R and Parrinello M 1985 *Phys. Rev. Lett.* **55** 2471
[6] Marzari N and Vanderbilt D 1997 *Phys. Rev.* B **56** 12847
[7] Marks N A, McKenzie D R, Pailthorpe B A, Bernasconi M and Parrinello M 1996 *Phys. Rev.* B **54** 9703
[8] McCulloch D G, McKenzie D R and Goringe C M 2000 *Phys. Rev.* B **61** 2349
[9] Silvestrelli P L, Marzari N, Vanderbilt D and Parrinello M 1998 *Solid State Commun.* **107** 7
[10] Fornari M, Marzari N, Peressi M and Baldereschi A 2001 *Comput. Mater. Sci.* **20** 337
[11] Hohenberg P and Kohn W 1964 *Phys. Rev.* B **136** 864
[12] Kohn W and Sham L J 1965 *Phys. Rev.* A **140** 1133
[13] Becke A D 1988 *Phys. Rev.* A **38** 3098
Lee C L, Yang W and Parr R G 1988 *Phys. Rev.* B **37** 785
[14] Kleinman L and Bylander D M 1982 *Phys. Rev. Lett.* **48** 1425
[15] MPI fur Festkorperforschung, IBM Zurich Research LaboratoryHutter J, Alavi A, Deutsch T, Bernasconi M, Goedecker S, Marx D, Tuckerman M and Parrinello M 1995–2001 *CPMD*
[16] Conde J P, Chu V, da Silva M F, Kling A, Dai Z, Soares J C, Arekat S, Federov A, Berberan-Santos M N, Giogis F and Pirri C F 1999 *J. Appl. Phys.* **85** 3327
[17] Kohn W 1959 *Phys. Rev.* **115** 809
[18] He L and Vanderbilt D 2001 *Phys. Rev. Lett.* **86** 5341
[19] Resta R 1998 *Phys. Rev. Lett.* **80** 1800